J. Vis. Commun. Image R. 24 (2013) 499–508

Contents lists available at SciVerse ScienceDirect

J. Vis. Commun. Image R.

journal homepage: www.elsevier.com/locate/jvci

# Stretchability-aware block scaling for image retargeting

Huan Du [a], Zhi Liu [a,b,c,*], Jianliang Jiang [a], Liquan Shen [a,c]

[a] School of Communication and Information Engineering, Shanghai University, Shanghai 200072, China
[b] IRISA, Campus Universitaire de Beaulieu, Rennes 35042, France
[c] Key Laboratory of Advanced Display and System Application, Shanghai University, Ministry of Education, Shanghai 200072, China

ARTICLE INFO

*Article history:*
Received 26 April 2012
Accepted 3 March 2013
Available online 21 March 2013

*Keywords:*
Block scaling
Image retargeting
Stretchability
Stretchable space
Block partition
Saliency
Scaling factor
User study

ABSTRACT

This paper proposes an efficient approach to retarget images based on stretchability-aware block scaling. The image stretchability is first evaluated based on gradient, saliency and color features, and is used to generate the stretchable space. Then the optimal size of the stretched image is determined under the constraint of stretchable space and the same aspect ratio as the target image. Based on the analysis of image stretchability measures, the original image is partitioned into non-stretchable blocks and stretchable blocks, and their scaling factors are calculated based on their stretchability measures and the stretched image size, in order to possibly preserve non-stretchable blocks without distortion and reasonably resize stretchable blocks. Finally, the stretched image is uniformly scaled to generate the target image. Experimental results on a variety of images and the user study demonstrate that our approach achieves an overall better retargeting performance compared to the state-of-the-art image retargeting approaches.



## 1. Introduction

With the emergence of a variety of intelligent devices, image retargeting has become more and more indispensable to efficiently display images on various displays with different sizes. Uniform scaling is the most widely used retargeting method due to its ease of implementation and higher runtime efficiency, but it is content-blind and may easily cause the deformation of the important content. Cropping [1–4] is a simple content-aware image retargeting approach, but it can be only used for reduction of image size and cannot efficiently deal with the image containing multiple objects scattered in the scene. Segmentation-based approaches [5,6] first segment the image into different object regions, then scale each region based on its importance, and finally recompose these scaled regions to generate the retargeted image. Although segmentation-based approaches can efficiently handle multiple objects, their performance highly depends on the quality of image segmentation results, and in many cases, it is not reliable to accurately segment different objects without any user interaction.

Warping is another commonly used content-aware retargeting approach with continuous operations. Warping based retargeting approaches non-uniformly scale different regions based on their importance measures to minimize the distortions on important regions. Different schemes such as nonlinear fisheye-view warping [7], similarity transformation based warping [8] and non-homogeneous warping [9] have been proposed to warp the image to the target size. In Ref. [10], a scale-and-stretch method is proposed to uniformly scale important regions and allow homogeneous regions to be distorted. Starting from different forms of partition on the input image, patch re-assembling method [11], Fourier analysis based scaling [12], quadtree based grid adjustment [13], and image distance based optimization [14] are efficiently exploited to generate the target image. In Ref. [15], a rectangular-block partitioning based scheme is proposed to first perform the constrained growth of rectangular regions containing important objects, and then perform rectangle partitioning and mapping on the remaining regions to generate the target image. These warping based approaches usually generate smooth retargeting results, but may incur noticeable distortions on background regions or around the object contours.

As a novel content-aware retargeting approach with discrete operations, seam carving [16] was firstly proposed by Avidan and Shamir. They use dynamic programming to find 8-connected seams with the lowest energy and delete/duplicate these seams to gradually reduce/expand the image size. Rubinstein et al. then presented the improved seam carving method [17] with the introduction of forward energy and graph cuts to improve the retargeting quality of seam carving. Later, different extensions to seam carving including seamlets based on discrete wavelet transform [18], importance diffusion scheme [19] and texture-aware salient edge model [20] are exploited to possibly avoid seams passing

* Corresponding author. Fax: +86 21 56331194.
*E-mail address:* liuzhisjtu@163.com (Z. Liu).

1047-3203/$ - see front matter © 2013 Elsevier Inc. All rights reserved.
http://dx.doi.org/10.1016/j.jvcir.2013.03.003

through important objects and excessively passing through some regions with the lower importance. In order to improve the computational efficiency of seam carving, seam update and seam split are jointly exploited to simultaneously search multiple seams [21]. However, when the retargeting ratio is higher, seams have to pass through some important object regions, and thus noticeable distortions are unavoidably incurred using these seam carving based approaches.

Considering that any retargeting approach cannot always perform well on images with different contents, a multi-operator approach [22], which combines three operations, i.e., scaling, cropping and seam carving, is proposed to generate the retargeting result by optimizing an image-to-image similarity measure called bidirectional warping. Inspired by the concept of multiple operations, seam carving and scaling [23,24], warping and scaling [25] are combined with different schemes to obtain a generally better retargeting result than individual operation. However, the shortcoming of each individual operation may still degrade the retargeting quality when the image is shrunk or enlarged too much.

In this paper, we propose an efficient image retargeting approach based on stretchability-aware block scaling. The main contribution of our approach is threefold. First, we propose to evaluate the image stretchability based on gradient, saliency and color features, and exploit the image stretchability to direct the retargeting process. Second, we propose the concept of stretchable space, which indicates the suitable range of non-uniform shrinkage/enlargement on the original image, to determine the optimal size of the stretched image. Finally, the analysis of stretchability measures is exploited to partition the image into stretchable blocks and non-stretchable blocks, and reasonably determine their scaling factors. Due to the above mentioned three characteristics, our approach adapts well to different types of images and achieves the overall better retargeting performance.

The rest of this paper is organized as follows. Section 2 describes the proposed retargeting approach in detail. Experimental results are presented in Section 3, and conclusions are given in Section 4.

## 2. The proposed retargeting approach

To retarget an original image $I_o$ with size $W_o \times H_o$ to a target image $I_t$ with size $W_t \times H_t$, we first calculate the stretchability rate of the original image based on three cues, i.e., gradient, saliency and color. Then we generate the stretchable space to determine the optimal size $W_s \times H_s$ of the stretched image $I_s$, which has the same aspect ratio with the target image. Next, we partition the original image into several blocks based on the analysis of stretchability rate, and use block scaling to obtain the stretched image. Finally, we perform the uniform scaling on the stretched image to generate the target image.

### 2.1. Image stretchability

The important content in most images can be generally identified based on the cues of gradient, saliency and color, and thus we calculate the stretchability rate of the image on the three aspects. We estimate the stretchability rate in the horizontal and vertical direction, respectively. Take the horizontal direction for an example, the stretchability of each column is defined as

$$r_h(j) = \omega_1 r_h^g(j) + \omega_2 r_h^s(j) + \omega_3 r_h^c(j) \tag{1}$$

where $r_h^g(j)$, $r_h^s(j)$ and $r_h^c(j)$ denote the stretchability of the $j$th column in terms of gradient, saliency and color, respectively. Specifically, they are defined as follows:

$$r_h^g(j) = \max\left\{\left\{\overline{G_h^{\max}} - \max_i[g(i,j)]\right\}, 0\right\} \tag{2}$$

where $g(i,j)$ denotes the gradient magnitude of the pixel $p(i,j)$, which locates at the $i$th row and the $j$th column, and $\overline{G_h^{\max}} = (1/W_o)\cdot\sum_{j=1}^{W_o}\max[g(i,j)]$ denotes the average of the column-wise maximal gradient values. Eq. (2) indicates that the stretchability rate of each column is smaller if the maximal gradient value in the column is higher, and thus the stretchability rates of the columns in the smooth regions are higher than those in the structured regions.

$$r_h^s(j) = \max\left\{\left(\frac{1}{W_o}\sum_{j=1}^{W_o} S_j\right) - S_j, 0\right\} \tag{3}$$

where the sum of saliency values in the $j$th column is denoted by $S_j = \sum_{i=1}^{H_o} s(i,j)$, and $s(i,j)$ is the saliency value at each pixel $p(i,j)$. We use the nonparametric saliency model in [26] to generate the saliency map. Similarly as Eq. (2), in terms of saliency, Eq. (3) lowers the stretchability rate of the column with a higher sum of saliency values.

$$r_h^c(j) = \frac{1}{H_o}\sum_{i=1}^{H_o}\frac{1}{D(\mathbf{c}_{i,j-1},\mathbf{c}_{i,j}) + D(\mathbf{c}_{i,j},\mathbf{c}_{i,j+1}) + \alpha} \tag{4}$$

where $\mathbf{c}_{i,j}$ denotes the color feature vector at each pixel $p(i,j)$, $D(\mathbf{c}_{i,j-1},\mathbf{c}_{i,j})$ denotes the Euclidean distance between $\mathbf{c}_{i,j-1}$ and $\mathbf{c}_{i,j}$, and $\alpha$ is set to a very small value, 1e−5, to avoid division by zero. It can be seen from Eq. (4) that the column showing a similar color with its neighboring columns is assigned with a higher stretchability.

After the calculation of $r_h^g(j)$, $r_h^s(j)$ and $r_h^c(j)$ using Eqs. (2)–(4), the three terms are respectively normalized into the same range of [0,1]. Specially, the normalized value for $r_h^g(j)$ is $(r_h^g(j) - r_{\min}^g)/(r_{\max}^g - r_{\min}^g)$, where $r_{\max}^g$ and $r_{\min}^g$ denote the maximum and the minimum, respectively, in $r_h^g$. Similar normalization functions are also used for $r_h^s(j)$ and $r_h^c(j)$. The three weights are set proportional to the corresponding sum of stretchability rates as follows:

$$\omega_1 = \frac{\sum_j r_h^g(j)}{\sum_j r_h^g(j) + \sum_j r_h^s(j) + \sum_j r_h^c(j)},$$
$$\omega_2 = \frac{\sum_j r_h^s(j)}{\sum_j r_h^g(j) + \sum_j r_h^s(j) + \sum_j r_h^c(j)},$$
$$\omega_3 = \frac{\sum_j r_h^c(j)}{\sum_j r_h^g(j) + \sum_j r_h^s(j) + \sum_j r_h^c(j)}$$

Based on the stretchability rate of each column, the overall stretchability measure in the horizontal direction is defined as

$$\Re_h = \frac{1}{W_o}\sum_{j=1}^{W_o} r_h(j) \tag{5}$$

For the example image in Fig. 1, the stretchability rates of columns in terms of gradient, saliency and color are calculated and shown using the heat maps from the 1st to the 3rd row in Fig. 1(a), and then the column-wise stretchability map is generated based on Eq. (1) and shown in the 4th row of Fig. 1(a). In these heat maps, a warmer/colder color indicates a higher/lower stretchability of each column, and we can see from the column-wise stretchability map that the stretchability of human object regions is obviously lower than background regions.

### 2.2. Stretchable space

The optimal size $W_s \times H_s$ of the stretched image $I_s$ is determined under the constraint of aspect ratio, i.e., $W_s/H_s = W_t/H_t = \tau_t$, so that the uniform scaling can be finally used to resize the stretched image to the target size $W_t \times H_t$. Based on the two overall

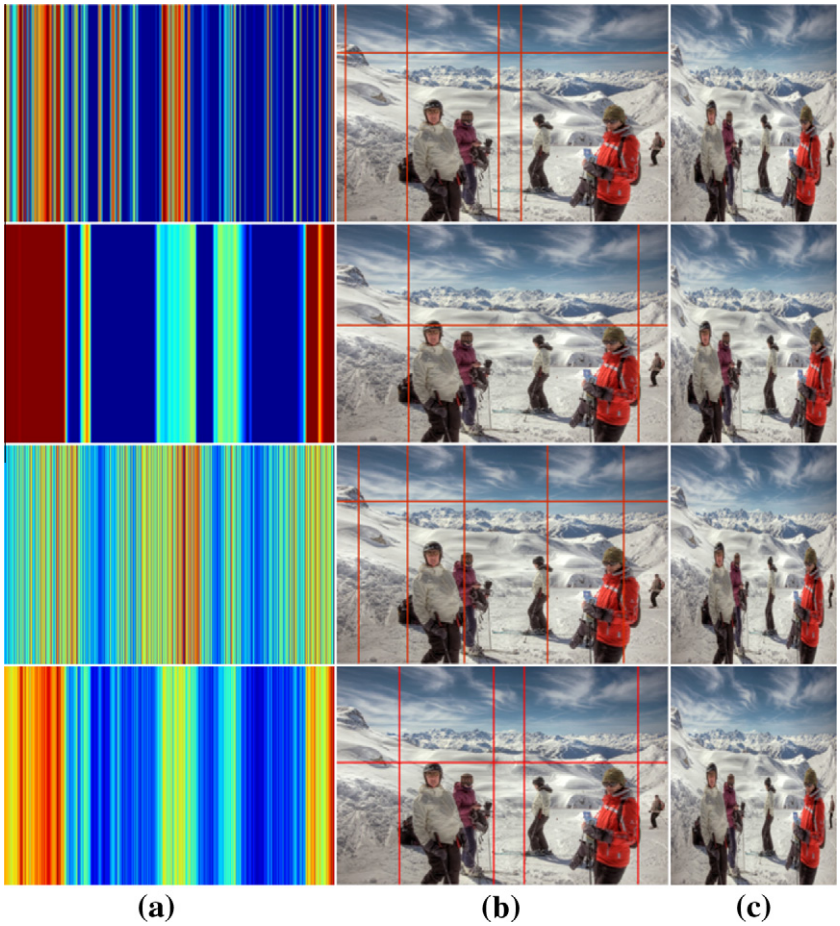


**Fig. 1.** (a) The heat maps representing stretchability rates in terms of gradient (the 1st row), saliency (the 2nd row), color (the 3rd row), and the column-wise stretchability map (the 4th row). (b) Image partition results generated based on the corresponding stretchability rates. (c) Retargeting results generated using our approach to reduce the image width by 50%.

stretchability rates, $\Re_h$ in the horizontal direction and $\Re_v$ in the vertical direction, the stretchable space of the original image is defined as

$$\begin{cases} W_o(1-\Re_h) \leqslant w \leqslant W_o(1+\Re_h) \\ H_o(1-\Re_v) \leqslant h \leqslant H_o(1+\Re_v) \end{cases} \tag{6}$$

where $(w,h)$ denotes any point in the stretchable space. As shown in Fig. 2(a), the constraint line of target aspect ratio is the blue line with the slope of $\tau_t$, and the red line is with the slope of original aspect ratio, $\tau_o = W_o/H_o$. The blue point denotes the size of the original image, and the purple rectangle denotes the stretchable space $R$, which consists of four sub-regions, i.e., $R1$, $R2$, $R3$ and $R4$, respectively.

In order to shrink or enlarge the original image as uniformly as possible, we consider the above aspect ratio constraint to search the optimal size point by minimizing the absolute difference between the original aspect ratio and the aspect ratio of the reduced/expanded size, i.e., $(w - W_o)/(h - H_o)$. Explicitly, the optimal width $W_s$ and the optimal height $H_s$ of the stretched image are determined as follows:

$$\begin{aligned} (W_s, H_s) &= \arg\min_{(w,h)\in R} \left\{ \left| \frac{w-W_o}{h-H_o} - \frac{W_o}{H_o} \right| \right\} \\ s.t.\ & W_s/H_s = W_t/H_t = \tau_t \end{aligned} \tag{7}$$

Using Eq. (7), the optimal size $(W_s,H_s)$ is selected as the yellow point in Fig. 2(a). It is noteworthy that the optimal size point lies in the sub-region $R1$ or $R4$, unless the blue line intersects with none of them. Due to the concurrently shrinking/enlarging in both

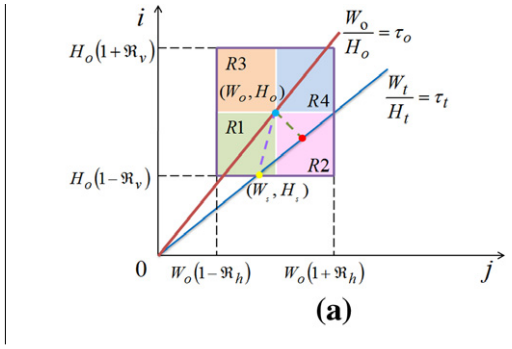


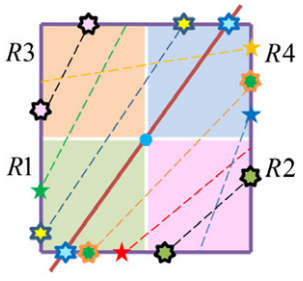


| | R1 | R2 | R3 | R4 | optimal size |
|---|---|---|---|---|---|
| case1 | √ | √ | | | ★ |
| case2 | √ | √ | | √ | ✹ |
| case3 | √ | | √ | | ★ |
| case4 | √ | | √ | √ | ✡ |
| case5 | | | √ | √ | ★ |
| case6 | | | √ | | ✡ |
| case7 | | √ | | √ | ★ |
| case8 | | √ | | | ✹ |
| case9 | √ | | | √ | ✡ |

(b)

**Fig. 2.** (a) Illustration of the stretchable space. (b) Schematic map of intersection cases.

directions in $R1/R4$, the image structure can be better preserved with less shape distortion. In contrast, if the optimal size point in Fig. 2(a) is selected as the red point, which has the least difference with the original size, it will obviously incur structural distortion because the red point falls into $R2$, which shrinks in the vertical direction while enlarges in the horizontal direction. For completeness, Fig. 2(b) illustrates all the 9 cases of intersection between the constraint line of aspect ratio and the stretchable space, and the optimal size determined in each case. It should be noted that in the case of 2, 4, 6, 8 and 9, there are two intersection points as shown in Fig. 2(b), and Eq. (7) is used to determine which one is the optimal size.

### 2.3. Partition

Based on the stretchability rates and the optimal size of the stretched image obtained in the previous two subsections, the original image is partitioned into several blocks. The following will mainly describe the partition process in the horizontal direction, and the partition process in the vertical direction can be performed in a similar way. We use the overall stretchability measure in the horizontal direction, $\Re_h$, as the threshold, to classify each column into either stretchable region $\Im$ or non-stretchable region $\aleph$ as follows:

$$\begin{aligned} &\forall i \in [1, H_o], p(i,j) \in \Im, if\ r_h(j) \geqslant \Re_h \\ &\forall i \in [1, H_o], p(i,j) \in \aleph, otherwise \end{aligned} \tag{8}$$

The stretchability rates $r_h(j)$ of all columns are first plotted as the original stretchability curve, and a mean filter with the window width of $W_o/N_B$ is then exploited to obtain the smoothed stretchability curve. $N_B$ is set to 7, a moderate value determined by our experiments. As shown in Fig. 3, the smoothed curve of $r_h(j)$ is shown using the green curve, and the threshold $\Re_h$ is marked using the blue line. Using Eq. (8) for classification, the adjacent columns belonging to stretchable region or non-stretchable region constitute each block accordingly. A similar analysis is also performed on the stretchability rates $r_v(i)$ of all rows. For example, Fig. 3 shows a block partition with 5 blocks in the horizontal direction and 2 blocks in the vertical direction, and we can see that different human objects are reasonably put into different blocks.

For a visually comparison, the image partition result in Fig. 3 is also shown in the bottom row of Fig. 1(b), and the image partition results based on the stretchability rates of gradient, saliency and color, respectively, are shown in the top three rows of Fig. 1(b). We can observe from Fig. 1(b) that the image partition result generated based on the column-wise and row-wise stretchability maps, which are calculated by integrating the features of gradient, saliency and color, is more reasonable than the other three partition results.

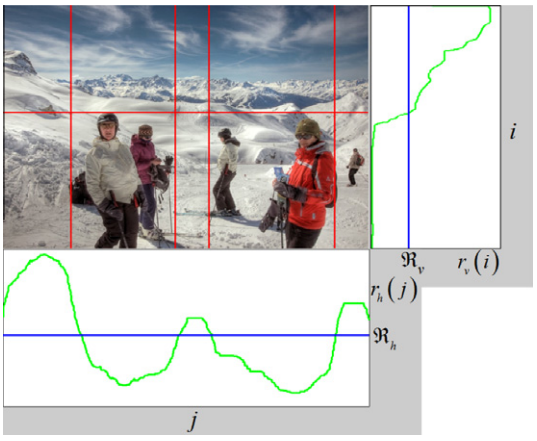


**Fig. 3.** Illustration of stretchability based image partition.

Assume that there are $K$ blocks, $B_k (k = 1, \ldots, K)$, in the horizontal direction, the stretchability rate of each block $B_k$ is defined as

$$br_k = \frac{\sum_{j \in B_k} r_h(j)}{BW_k} \tag{9}$$

where $BW_k$ is the width of the block $B_k$.

### 2.4. Block scaling

For a clear description, the total width of non-stretchable blocks is denoted by $W_\aleph = \sum_{B_k \in \aleph} BW_k$. In the case of $W_\aleph < W_s$, it is possible to keep non-stretchable blocks unchanged by setting the scaling factor of non-stretchable blocks to 1. Besides, it is reasonable that we also need to guarantee that the scaling of stretchable blocks is in the stretchable range, i.e., $W_s - W_\aleph > \sum_{B_l \in \Im} (1 - br_l) \cdot BW_l$, and the scaling factor of each stretchable block should be determined based on its stretchability rate. Specifically, the scaling factor $s_k$ of each block $B_k$ is defined as

$$s_k = \begin{cases} 1, & B_k \in \aleph \\ \frac{W_s - W_\aleph}{\sum_{B_l \in \Im} (1 - br_l) \cdot BW_l} \cdot (1 - br_k), & B_k \in \Im \end{cases} \tag{10}$$

It can be seen from Eq. (10) that the scaling factor $s_k$ of each stretchable block $B_k$ is determined based on the two terms. The first term with the fractional form reflects the overall margin for stretching the image, i.e., a higher value indicates a larger margin for stretching the whole image, and the second term $(1 - br_k)$ is a block-dependent term, which can be considered as the block's non-stretchability rate, i.e., the scaling factor of a block with a smaller stretchability rate is closer to 1.

In the other case of $W_s - W_\aleph \leqslant \sum_{B_l \in \Im} (1 - br_l) \cdot BW_l$, it is not enough to only scale stretchable blocks to obtain the stretched image, and non-stretchable blocks should also be scaled to avoid excessive scaling of stretchable blocks. Therefore, for both stretchable blocks and non-stretchable blocks, the scaling factor of each block $B_k$ is defined as

$$s_k = \frac{W_s}{\sum_{B_l \in \Im, \aleph} (1 - br_l) \cdot BW_l} \cdot (1 - br_k), \quad B_k \in \Im, \aleph \tag{11}$$

Using Eq. (10) or (11), each block $B_k$ is scaled based on its scaling factor $s_k$, and the sum of the width of all scaled blocks equals to the determined width of the stretched image, i.e., $\sum_k s_k \cdot BW_k = W_s$. Since the stretched image has the same aspect ratio with the target image, the uniform scaling is finally performed on the stretched image to generate the target image.

Based on the different partition results shown in Fig. 1(b), the retargeting results with a width reduction of 50% generated using the proposed block scaling scheme are shown in Fig. 1(c). We can further observe from Fig. 1(c) that the integration of gradient, saliency and color features is effective for image retargeting.

For the example image with the size of $1004 \times 661$ shown in Fig. 4(a), we use our retargeting approach to reduce its width by 10%, 15%, 35% and 50%, respectively. When the target size is in the stretchable range such as the cases of Fig. 4(b) and (c), the background regions are shrunk while the aspect ratio of salient objects is preserved well. However, when the target size is out of the stretchable range such as the cases of Fig. 4(d) and (e), our approach has to gradually shrink salient object regions. Nonetheless, in the case that our approach cannot keep the aspect ratio of salient objects, our approach can still achieve a better retargeting result than other retargeting approaches as shown in Fig. 5. For a visual comparison, the retargeting results with a width reduction


**Fig. 4.** (a) The original image and retargeting results generated using our approach to reduce the image width by (b) 10%, (c) 15%, (d) 35% and (e) 50%.


**Fig. 5.** Retargeting results generated using (a) ISC, (b) WARP, (c) SNS, (d) MULTIOP and (e) our approach to reduce the image width by 50%.

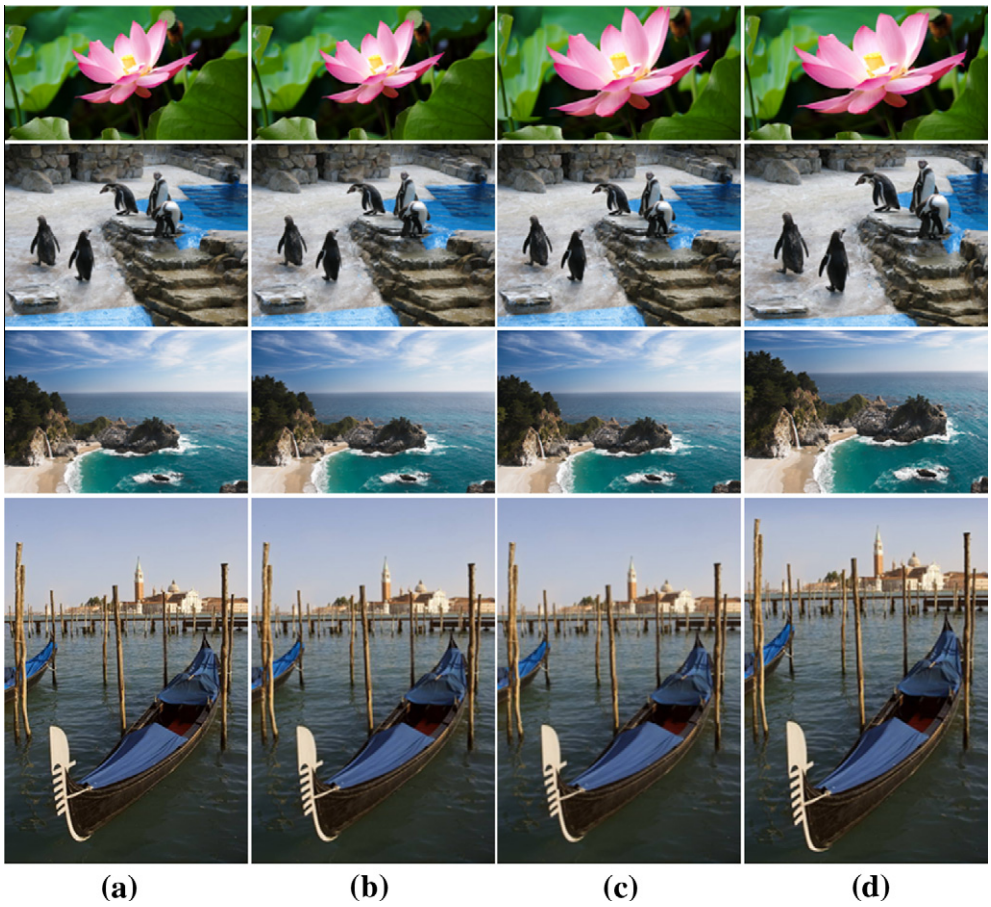


**Fig. 6.** (a) Original image thumbnails (both width and height are resized to a half of the original images), and retargeting results generated using (b) scaling, (c) Pal's approach and (d) our approach to reduce both width and height by 50%.

of 50% generated using the improved seam carving (ISC) [17], the non-homogeneous warping (WARP) [9], the scale-and-stretch method (SNS) [10], the multi-operator (MULTIOP) [22] and our approach are shown in Fig. 5(a)–(e), respectively. We can see from Fig. 5(a) that ISC results in noticeable artifacts on human body due that some seams unduly pass through the regions containing humans, and observe from Fig. 5(c) that SNS excessively enlarges background and results in too small salient objects. Compared with

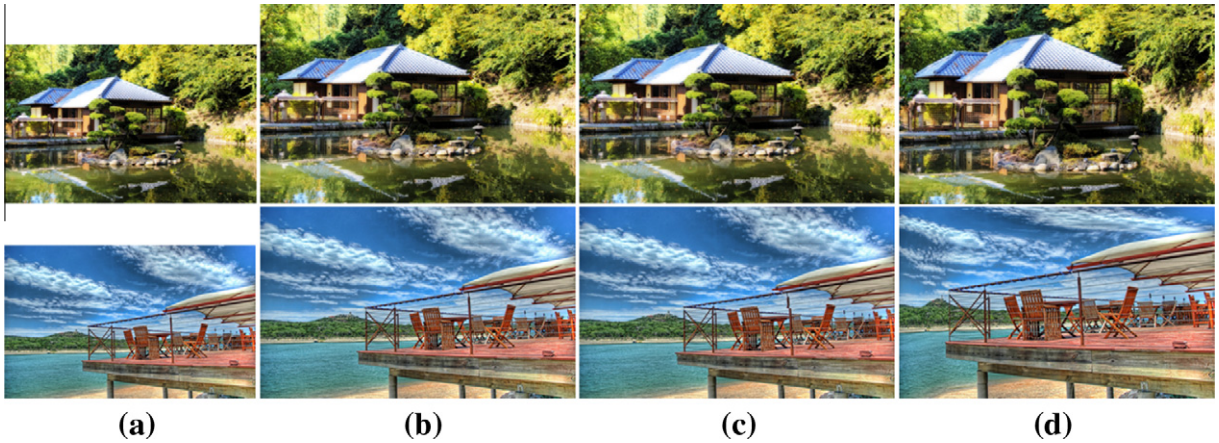


**Fig. 7.** (a) Original images and retargeting results generated using (b) scaling, (c) Pal's approach and (d) our approach to increase both width and height by 25%.


**Fig. 8.** (a) Original image and the retargeting results generated using (b) ISC, (c) WARP, (d) SNS, (e) MULTIOP and (f) our approach to reduce the image width by 50%.

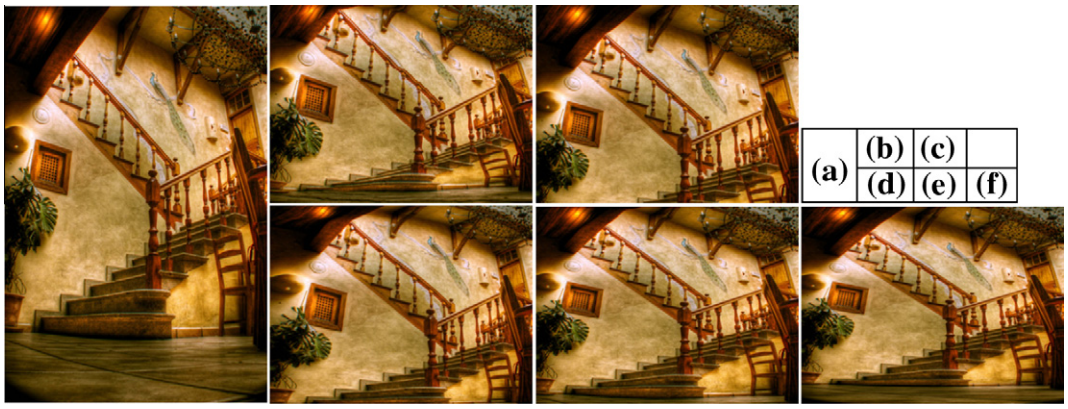


**Fig. 9.** (a) Original image and the retargeting results generated using (b) ISC, (c) WARP, (d) SNS, (e) MULTIOP and (f) our approach to reduce the image height by 50%.

ISC and SNS, the retargeting results obtained using WARP and MULTIOP show the better visual quality, but they also introduce obvious distortion on the leftmost person. Besides, as shown in Fig. 5(d), the rightmost person is also cut off due to the cropping operation combined in MULTIOP. Compared with the other four approaches, our approach can make a better balance between pro-

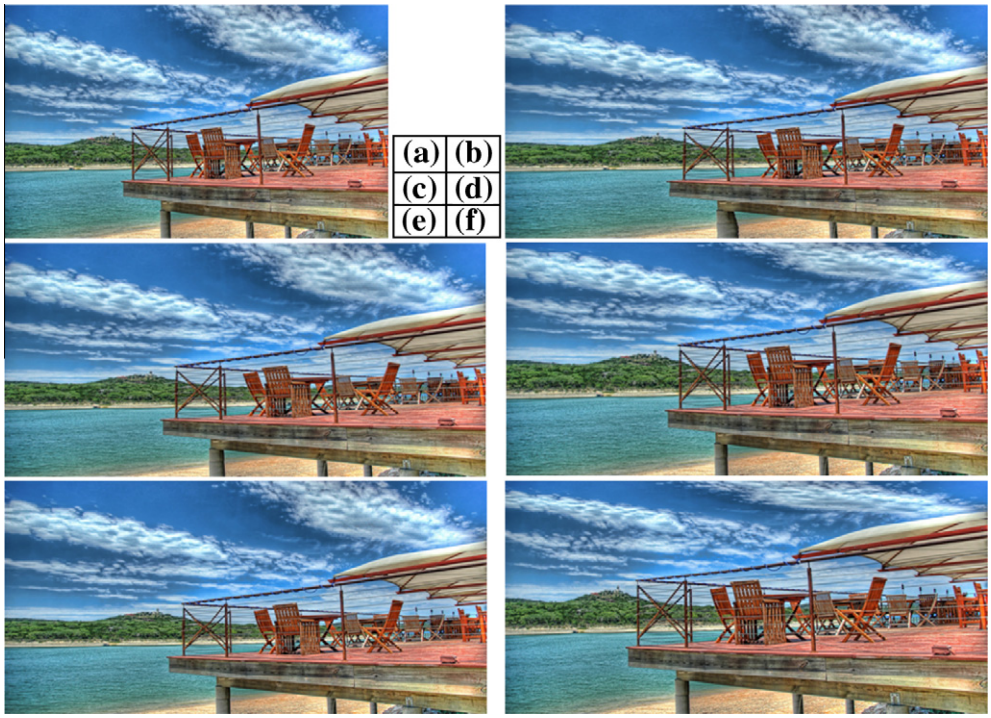


**Fig. 10.** (a) Original image and the retargeting results generated using (b) ISC, (c) WARP, (d) SNS, (e) MULTIOP and (f) our approach to increase the image width by 25%.

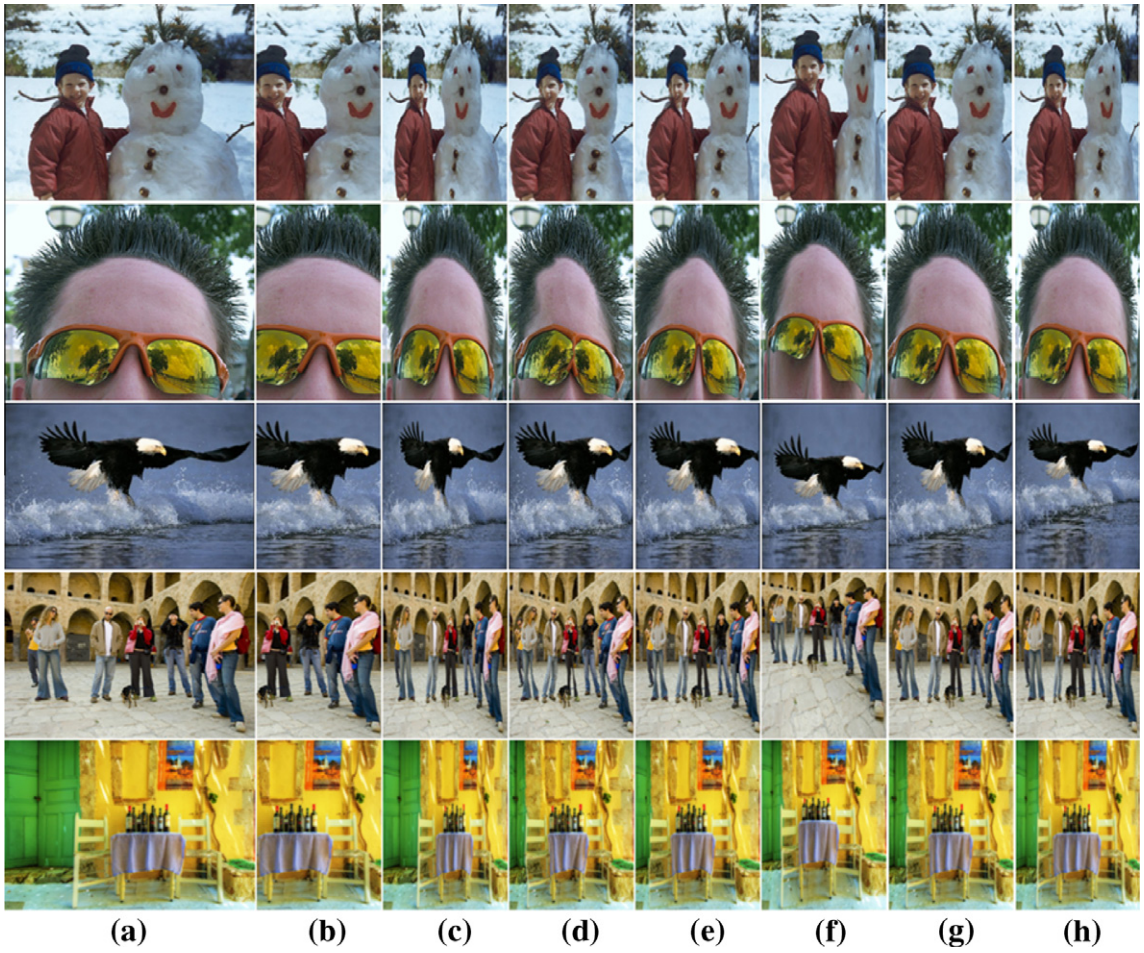


**Fig. 11.** (a) More test images and the retargeting results generated using (b) cropping, (c) scaling, (d) ISC, (e) WARP, (f) SNS, (g) MULTIOP and (h) our approach to reduce the image width by 50%.


**Fig. 12.** Comparison of retargeting results with width reduction by 50%. (a) Original image, (b) ISC, (c) WARP, (d) SNS, (e) MULTIOP and (f) our approach.

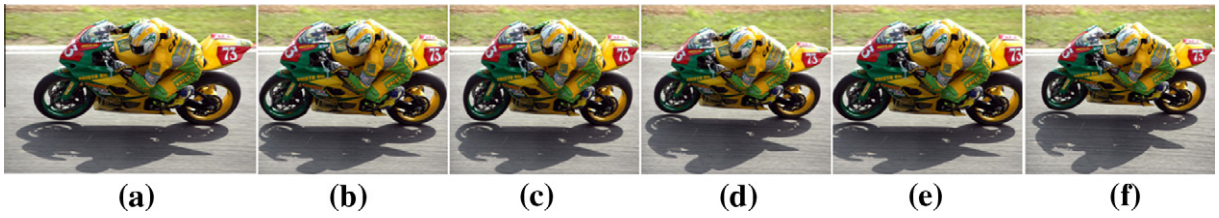


**Fig. 13.** Comparison of retargeting results with width reduction by 25%. (a) Original image, (b) ISC, (c) WARP, (d) SNS, (e) MULTIOP and (f) our approach.

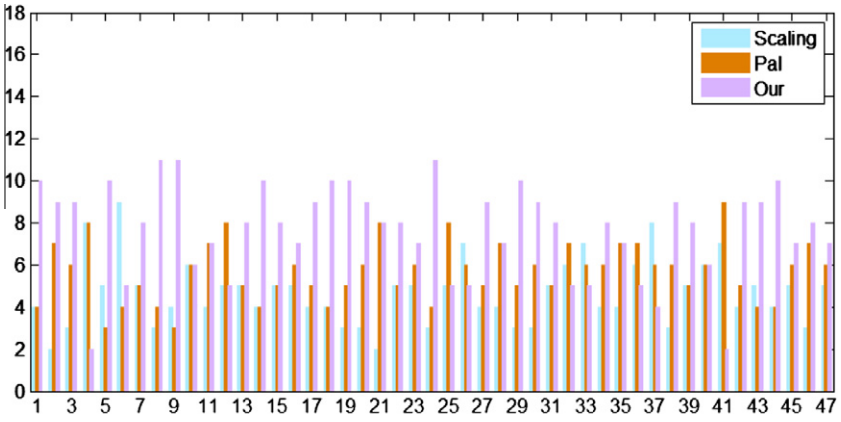


**Fig. 14.** Voting results on each test image in the case of keeping the aspect ratio.

tecting the content integrity of the image and preserving the important objects, and thus shows an overall better visual quality.

## 3. Experimental results

In order to evaluate the retargeting performance of our approach, we have performed experiments on a variety of test images from the image retargeting dataset [27], which can be downloaded from http://people.csail.mit.edu/mrub/retargetme/download.html. Considering that the target size may have the same or different aspect ratio compared with the original size, we performed two sets of experiments and comparisons as follows.

In the case of keeping the same aspect ratio as the original size, we compare our approach with scaling and Pal's approach [15]. Fig. 6 shows several examples of reducing both width and height by 50%, and Fig. 7 shows several examples of increasing both width and height by 25%. As a simple operation, scaling can effectively retarget images containing uniform regions. However, it is content-blind and salient objects cannot be emphasized in the retargeting results (see Fig. 6(b) and Fig. 7(b)). Compared with scaling, Pal's approach can highlight salient objects more effectively (see the lotus in the 1st row and the ship in the 4th row of Fig. 6(c)). However, when there are several objects or complex background regions, the retargeting results generated using Pal's approach are similar with that generated using scaling (see the penguins and the mountain in the 2nd and 3rd row of Fig. 6(c), as well as the pavilions and the platform in the two rows of Fig. 7(c)). Com-

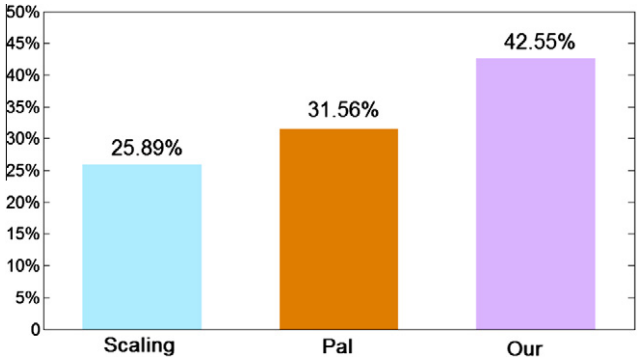


**Fig. 15.** Overall voting results of the three retargeting approaches in the case of keeping the aspect ratio.

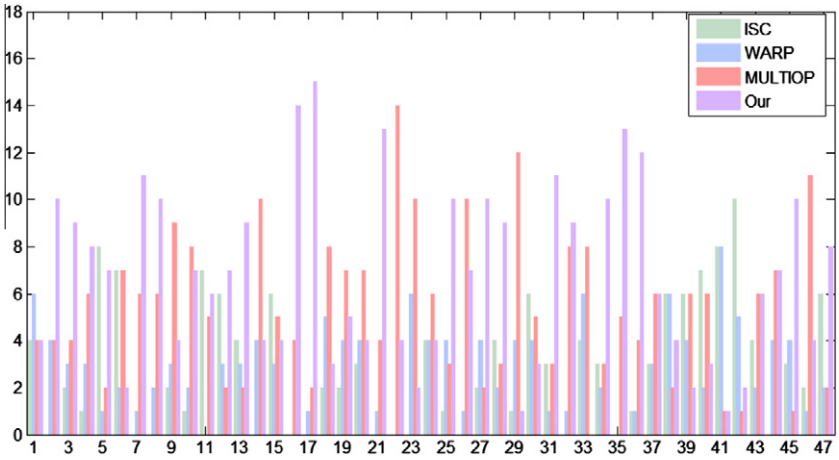


**Fig. 16.** Voting results on each test image in the case of changing the aspect ratio.

pared with scaling and Pal's approach, we can observe from Fig. 6(d) and Fig. 7(d) that our approach generally achieves the better retargeting results, in which these salient objects are reasonably highlighted.

In the case of changing the aspect ratio, we compare our approach with four representative retargeting approaches, i.e., ISC [17] as a discrete approach, WARP [9] and SNS [10] as continuous approaches, and MULTIOP [22] as a hybrid approach combining both discrete and continuous operations. All the retargeting results of the four approaches are provided by the image retargeting dataset [27]. Figs. 8 and 9 show two examples of reducing image width and height, respectively, and Fig. 10 shows an example of image enlargement. As a flexible operation using seams, ISC can effectively retarget images containing uniform or highly textured background regions. However, ISC usually results in noticeable distortions on important objects or structured background regions (see the roof in Fig. 8(b) and the staircase in Fig. 9(b)) due to its discrete nature, especially when the retargeting ratio is relatively higher such as 50% or even more. WARP can better maintain the smoothness of the retargeted image, but it is also likely to cause significant distortions on important objects and structured regions (see the roof in Fig. 8(c), and the upper left roof in Fig. 9(c)) when the retargeting ratio is relatively higher. SNS usually preserves salient objects well, but sometimes it excessively stretches background regions and thus cannot effectively highlight salient objects (see the pavilions in Fig. 8(d)). Compared with ISC, WARP and SNS, MULTIOP and our approach generally perform better on most images, and usually obtain the retargeting results with similar visual quality as shown in Fig. 8(e) and (f) and Fig. 9(e) and (f). Compared with MULTIOP that combines cropping, scaling and seam carving, our approach is much simpler yet effective to preserve the important content and the scene integrity well due to the use of stretchability-aware block scaling. The example of image enlargement shown in Fig. 10 also demonstrates that our approach can sufficiently highlight the platform without noticeable distortions, and achieves a more visually pleasing result than other approaches.

The retargeting results on more test images including human faces, animals, and indoor/outdoor photos are shown in Fig. 11, in which the results obtained using the other two simple approaches, i.e., cropping and uniform scaling, are also shown for a visual comparison. We can observe from Fig. 11(b) that the cropping approach may violate the scene integrity due to the complete or partial loss of informative content outside the cropping window. As shown in Fig. 11(c), uniform scaling approach can protect the scene integrity well, but have to excessively squeeze the important object regions. We can observe from Fig. 11(d)–(f) that noticeable distortions on some object regions, such as the child's face in the 1st row, the sunglasses in the 2nd row, the eagle's wing in the 3rd row, the legs in the 4th row, and the left chair in the 5th row, are usually incurred by ISC, WARP and SNS. Compared with the above five approaches, the results shown in Fig. 11(g) and (h) further demonstrate the better retargeting robustness of MULTIOP and our approach on various images.

However, for some images such as Fig. 12(a), in which the objects (houses) cover a majority part of the whole image, our approach generates the similar retargeting result as the uniform scaling. ISC, WARP and SNS introduce shape distortions on the edges of houses and/or the road boundaries, while MULTIOP generates a relatively better retargeting result with less shape distortions. Besides, the inaccurate partition sometimes results in the structure distortion in our retargeting result. As shown in Fig. 13(f), the structured region of the front wheel is distorted due to the small deviation in the partition. However, for such an image containing a relatively large structured object, ISC and WARP also introduce obvious distortions on the region of front wheel, and MULTIOP cuts part of the rear wheel due to the combination of cropping.

In order to objectively compare the retargeting performance of different approaches, we have conducted a user study on the retargeting results of all the 47 test images. A total of 18 participants (11 male and 7 female) were involved in the user study. Each original image was first displayed on the upper left part of

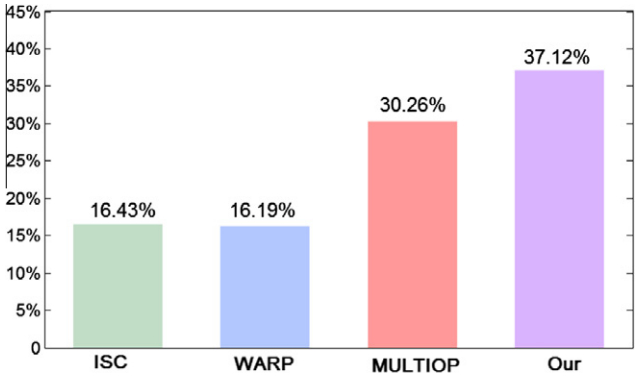


**Fig. 17.** Overall voting results of the four retargeting approaches in the case of changing the aspect ratio.

the screen as the reference, and the corresponding retargeted images were displayed in the random order below the original image. When the user moved the mouse over any retargeted image, the image was displayed more clearly on the upper right part of the screen. Each participant only needed to click on the most favorite retargeted image for each test image, and voted for all the 47 test images to finish the user study. In the case of keeping the aspect ratio, we compare our approach with scaling and Pal's approach. In the case of changing the aspect ratio, we choose ISC, WARP and MULTIOP as the representative of discrete approaches, continuous approaches and hybrid approaches, respectively, to compare with our approach. The voting results on each test image are shown in Figs. 14 and 16, respectively, for an image-wise comparison of these retargeting approaches, and the ratio of votes for each retargeting approach is shown in Figs. 15 and 17, respectively, as an overall performance comparison. We can observe from Figs. 14 and 16 that for all 47 images, our approach obtains the highest votes on 37 images and 23 images, respectively. We can also conclude from Figs. 15 and 17 that our approach achieves the overall better retargeting performance with the highest ratio of votes.

## 4. Conclusion

In this paper, we have presented an efficient approach to retarget images based on image stretchability, which is exploited to divide the image into different blocks. Non-stretchable blocks are possibly preserved without distortion, and stretchable blocks are reasonably scaled based on their stretchability measures. Besides, we also proposed the stretchable space to determine the suitable size of the stretched image. Experimental results on a variety of test images and the user study demonstrate the better retargeting performance of our approach. In our future work, we will try to explore the video stretchability and extend the block scaling to volume scaling for efficient video retargeting.

## Acknowledgments

This work was supported by Shanghai Natural Science Foundation (No. 11ZR1413000), National Natural Science Foundation of China under Grant No. 61171144, Innovation Program of Shanghai Municipal Education Commission (No. 12ZZ086), the Key (Key grant) Project of Chinese Ministry of Education (No. 212053) and the Innovation Program for Graduate Students of Shanghai University (No. SHUCX120134). The authors would like to thank the anonymous reviewers and the associate editor for their valuable comments, and also thank Dr. Pal for providing the research code for comparison.

## References

[1] L.Q. Chen, X. Xie, X. Fan, W.Y. Ma, H.J. Zhang, H.Q. Zhou, A visual attention model for adapting images on small displays, ACM Multimedia Syst. J. 9 (2003) 353–364.
[2] H. Liu, X. Xie, W.Y. Ma, H.J. Zhang, Automatic browsing of large pictures on mobile devices, in: Proc. ACM Multimedia, Berkeley, CA, USA, 2003, pp. 148–155.
[3] X. Fan, X. Xie, H.Q. Zhou, W.Y. Ma, Look into video frames on small displays, in: Proc. ACM Multimedia, Berkeley, CA, USA, 2003, pp. 247–250.
[4] A. Santella, M. Agrawala, D. Decarlo, D. Salesin, M. Cohen, Gaze-based interaction for semiautomatic photo cropping, in: Proc. CHI, Montreal, Quebec, Canada, 2006, pp. 771–780.
[5] V. Setlur, S. Takagi, R. Raskar, M. Gleicher, B. Gooch, Automatic image retargeting, in: Proc. MUM, Christchurch, New Zealand, 2005, pp. 59–68.
[6] W.H. Cheng, C.W. Wang, J.L. Wu, Video adaptation for small display based on content recomposition, IEEE Trans. Circuits Syst. Video Technol. 17 (2007) 43–58.
[7] F. Liu, M. Gleicher, Automatic image retargeting with fisheye-view warping, in: Proc. ACM Symp. UIST, Seattle, WA, USA, 2005, pp. 153–162.
[8] R. Gal, O. Sorkine, D. Cohen-Or, Feature-aware texturing, in: Proc. Eurograph. Symp. Rendering, Nicosia, Cyprus, 2006, pp. 297–303.
[9] L. Wolf, M. Guttmann, D. Cohen-or, Non-homogeneous content-driven video-retargeting, in: Proc. IEEE ICCV, Rio de Janeiro, Brazil, 2007, p. 4409010
[10] Y.S. Wang, C.L. Tai, O. Sorkine, T.Y. Lee, Optimized scale-and-stretch for image resizing, ACM Trans. Graphics 27 (2008) 118.
[11] T. S. Cho, M. Butman, S. Avidan, W. T. Freeman, The patch transform and its applications to image editing, in: Proc. IEEE CVPR, Anchorage, Alaska, USA, 2008, p. 4587642.
[12] J.S. Kim, J.H. Kim, C.S. Kim, Adaptive image and video retargeting technique based on Fourier analysis, in: Proc. IEEE CVPR, Miami, Florida, USA, 2009, pp. 1730–1737.
[13] B. Li, Y. Chen, J. Wang, L.Y. Duan, W. Gao, Fast retargeting with adaptive grid optimization, in: Proc. IEEE ICME, Barcelona, Spain, 2011, p. 6012050
[14] Y. Liang, Z. Su, X. Luo, Patchwise scaling method for content-aware image retargeting, Signal Process. 92 (2012) 1243–1257.
[15] R. Pal, J. Mukhopadhyay, P. Mitra, Image retargeting through constrained growth of important rectangular partitions, in: Proc. 4th International Conference on Pattern Recognition and Machine Intelligence, Moscow, Russia, 2011, pp. 104–109.
[16] S. Avidan, A. Shamir, Seam carving for content-aware image resizing, ACM Trans. Graphics 26 (2007) 10.
[17] M. Rubinstein, A. Shamir, S. Avidan, Improved seam carving for video retargeting, ACM Trans. Graphics 27 (2008) 16.
[18] D. Conger, H. Radha, M. Kumar, Seamlets: content-aware nonlinear wavelet transform, in: Proc. IEEE ICASSP, Dallas, Texas, USA, 2010, pp. 1450–1453.
[19] S. Cho, H. Choi, Y. Matsushita, S. Lee, Image retargeting using importance diffusion, in: Proc. IEEE ICIP, Cairo, Egypt, 2009, pp. 997–980.
[20] W. Kim, C. Kim, A texture-aware salient edge model for image retargeting, IEEE Signal Process. Lett. 18 (2011) 631–634.
[21] C.K. Chiang, S.F. Wang, Y.L. Chen, S.H. Lai, Fast JND-based video carving with GPU acceleration for real-time video retargeting, IEEE Trans. Circuits Syst. Video Technol. 19 (2009) 1588–1597.
[22] M. Rubinstein, A. Shamir, S. Avidan, Multi-operator media retargeting, ACM Trans. Graphics 28 (2009) 23.
[23] W. Dong, N. Zhou, J.C. Paul, X. Zhang, Optimized image resizing using seam carving and scaling, ACM Trans. Graphics 28 (2009) 125.
[24] Z. Liu, H. Yan, L. Shen, K.N. Ngan, Z. Zhang, Adaptive image retargeting using saliency-based continuous seam carving, Opt. Eng. 49 (2010) 017002.
[25] S.F. Wang, S.H. Lai, Compressibility-aware media retargeting with structure preserving, IEEE Trans. Image Process. 20 (2011) 855–865.
[26] Z. Liu, Y. Xue, L. Shen, Z. Zhang, Nonparametric saliency detection using kernel density estimation, in: Proc. IEEE ICIP, Hong Kong, China, 2010, pp. 253–256.
[27] M. Rubinstein, D. Gutierrez, O. Sorkine, A. Shamir, A comparative study of image retargeting, ACM Trans. Graphics 29 (2010) 160.